

Temperature Dependent Layer Breathing Modes in Two Dimensional Materials

Indrajit Maity, Prabal K Maiti, and Manish Jain*

Department of Physics, Indian Institute of Science, Bangalore-560012

(Dated: October 21, 2019)

Abstract

Relative out of plane displacements of the constituent layers of two dimensional materials gives rise to unique low frequency breathing modes. By computing the height-height correlation functions in momentum space, we show that, the layer breathing modes (LBMs) can be mapped consistently to vibrations of a simple linear chain model. Our calculated thickness dependence of LBM frequencies for few layer (FL) graphene and molybdenum disulphide (MoS_2) are in excellent agreement with available experiments. Our results show a redshift of LBM frequency with increase in temperature, which is a direct consequence of anharmonicities present in the interlayer interaction. We also predict the thickness and temperature dependence of LBM frequencies for FL hexagonal boron nitride (hBN). Our study provides a simple and efficient way to probe the interlayer interaction for layered materials and their heterostructures, with the inclusion of anharmonic effects.

Two dimensional (2D) materials, for example, graphene, transition metal dichalcogenides, hBN, are being studied extensively for their exciting electronic, thermal, mechanical properties [1, 2]. A great deal of effort has also been directed towards understanding hybrid structures of these 2D materials [3]. It is well known that, typically few layers of 2D materials and their hybrid structures are coupled by weak van der Waals (VDW) forces. Such layer-layer couplings give rise to unique low frequency *interlayer* vibrational modes at finite temperature, namely, shear and layer breathing modes (LBMs). [4, 5]. It has been found experimentally that, LBMs are more sensitive to external perturbations than shear modes [6]. These LBMs can be used as direct probe to determine layer thickness, stacking order, effects of external environment, adsorbates etc [6–18]. Furthermore, LBMs play a crucial role in interlayer electric conductance [19], thermoelectric transport [20]. Understanding the origin and quantification of LBM frequencies is thus of immense practical importance.

Three key features emerge from the low frequency Raman spectroscopic measurements of LBMs in 2D materials : (i) A system with n layers will have $n - 1$ *distinct* LBMs [21]. (ii) LBM frequencies (at the Γ point) are highly sensitive to the thickness of the material i.e. number of layers. For instance, when the number of layers of graphene is increased from 2 to 8, the lowest LBM frequency redshifts from 81 cm^{-1} to 22 cm^{-1} [6]. (iii) The lowest LBM frequency also redshifts with increment of temperature (T), as seen in experiments by controlled laser heating [6, 13]. The reported linewidths in Raman spectroscopic measurements for LBMs are typically larger than shear modes [11]. These observations suggest the presence of strong anharmonicity in the interlayer interaction for LBMs. In this work, we address these three key aspects of LBMs.

A 2D material embedded in 3D space can have out of plane acoustic phonon modes called flexural modes (ZA). In the harmonic approximation, these flexural modes have a dispersion, $\omega_{flex} \propto q^2$ for small momentum, q . For n layers, due to interlayer coupling, the degeneracy in ZA branch is lifted and *distinct* modes appear in the vibrational spectra, implying vertical stretching/compression of the layers. These modes are known as LBMs (ZO' , optical modes). In order to understand the thickness dependence of LBMs, two common approaches are used. First, a linear chain model of n masses with nearest neighbor interaction is used widely to determine LBM frequencies. This simple model has been shown to predict the frequencies accurately, given a knowledge of nearest neighbor layer coupling [6, 7, 10, 11]. However, the mapping of the n layer system to such a simple model

starting from a more general description of the constituent layers is unclear. The effects of next-nearest neighbor layer coupling in such a model have not been quantified as well. Second, first principles calculations based on density functional perturbation theory (DFPT) are frequently used to calculate LBM frequencies [10, 22]. In these calculations, however, the temperature dependence of LBMs is not revealed. The inclusion of anharmonic effects i.e. multi-phonon processes and thermal expansion coefficients are necessary to capture the temperature dependence of LBM frequencies.

Here, we present a simple method to calculate LBM frequencies by using a combination of classical molecular dynamics (MD) simulations and theory of membranes. We justify the application of linear chain model in the small momentum regime ($q \rightarrow 0$), by computing the height-height correlations. Our calculations of layer dependence of LBM frequencies for few-layer graphene and MoS₂ are in excellent agreement with available experiments. We show the evolution of LBM frequency with temperature for bilayer (BL) system of graphene, MoS₂ and hBN. In the studied temperature (T) range, we find expansion of interlayer separation and redshift in LBM frequency with T increment. As, the interlayer separation is calculated directly from MD simulation, *all* anharmonicities in the interlayer interaction are incorporated in the calculation.

We perform MD simulations with periodic boundary condition in the NPT ensemble using Nosé-Hoover thermostat and barostat as implemented in LAMMPS [23]. We simulate three different layered materials, namely, graphene, MoS₂, h-BN and vary the number of layers from 2 to 6. Initially, all the samples are chosen to be roughly square shaped and contain ≈ 8000 - 9000 atoms per layer (N). After equilibration, we use 4000 snapshots (2 nanosecond production run) to average the calculated properties. We use different forcefields (FFs) to compute LBM frequencies. For graphene three different FFs are adopted : Long Range Bond Order Potential for Carbon (LCBOP) [24], a combination of Reactive Empirical Bond Order potential and Lennard-Jones potential (REBO+LJ) [25, 26] and Dreiding, a more generic FF [27]. For the case of MoS₂ and hBN, a mix of Stillinger-Weber and Lennard-Jones potential (SW+LJ) [28–30] and Dreiding are used, respectively.

The applicability of the theory of membranes (a continuum description) to understand long-wavelength physics in 2D materials, such as graphene, is now well established [31–33]. In the harmonic approximation of membrane theory, the bending energy for a BL system

with weak VDW interaction between the layers, can be written as,

$$E_{BL} = \frac{1}{2} \int [\kappa(\nabla^2 h_1)^2 + \kappa(\nabla^2 h_2)^2 + \sigma(h_1 - h_2)^2] d^2x \quad (1)$$

where κ is the bending rigidity of each constituent layer, h_1, h_2 are heights of two layers with respect to each of their reference plane and σ denotes the interlayer coupling. In the momentum space, using the combinations $h = (h_1 + h_2)/\sqrt{2}$ and $\delta h = (h_1 - h_2)/\sqrt{2}$, one can identify two modes : *mean* and *fluctuation* mode. The corresponding height correlation functions [34], are

$$H^{BL}(q) = \langle |h(q)|^2 \rangle = \frac{Nk_B T}{S_0 \kappa q^4} \quad (2)$$

$$\delta H^{BL}(q) = \langle |\delta h(q)|^2 \rangle = \frac{Nk_B T}{S_0(\kappa q^4 + 2\sigma)} \quad (3)$$

where S_0 is the surface area per atom and $q = |\vec{q}|$, is defined by the dimension of the simulation box. The dispersion relations for the long-wavelength physics, can be inferred from the above relations : $\omega_{mean} = \sqrt{\frac{\kappa}{\rho}} q^2$ and $\omega_{fluc} = \sqrt{\frac{\kappa q^4 + 2\sigma}{\rho}}$, where ρ is the two dimensional mass density [See Supplementary Information (SI); Section A for single layer sheet and B for bilayer system]. It should be noted that, quantum effects are neglected in the calculation of height correlation functions ($H^{BL}(q), \delta H^{BL}(q)$). While the effects are important at low T , these effects are reported to be unimportant above a crossover temperature, $T^* \sim 70-90$ K [33]. All the correlation functions presented here, are calculated for $T \geq 150$ K, hence, quantum effects can be neglected.

Fig.1(a) shows height correlation functions per atom ($H^{BL}(q)/N, \delta H^{BL}(q)/N$) for the *mean* and *fluctuation* modes in BL graphene and MoS₂ at room temperature. In the figure we have shown the results for BL graphene using REBO+LJ and for BL MoS₂ using SW+LJ. However, the main features of the height correlation functions are insensitive to the choice of forcefields. The *mean* mode of BL graphene is well described within the harmonic approximation (Eqn.(2)) for $0.5\text{\AA}^{-1} \leq q \leq 1.0\text{\AA}^{-1}$. The membrane theory predicts a change in scaling, from $H^{BL}(q) \propto q^{-4}$ to $H^{BL}(q) \propto q^{-3.18}$, when anharmonicities become important owing to the coupling of bending and stretching [35]. This deviation from the harmonic approximations of membrane theory i.e. a change of scaling from $H^{BL}(q) \sim q^{-4}$, is found in all the simulated samples. Our results show that, anharmonic effects are more pronounced in BL MoS₂, compared to that of graphene (Fig.1(a)). More generally, we find *mean* mode of BL system behaves like a single layer for all the simulated materials . The

fluctuation mode for both BL graphene and MoS₂ becomes a constant for $q \lesssim 0.2\text{\AA}^{-1}$. This implies that near the zone center (Γ point) the interlayer coupling (σ) dictates the height fluctuations, as predicted by Eqn.(3). This aspect of the *fluctuation* mode is key for the rest of our work. Contrary to the *mean* mode, for small q , the anharmonicities arising from the coupling between bending and stretching are found to be irrelevant for the *fluctuation* mode. The *fluctuation* mode is identified with LBM. The Bragg peaks (Fig.1(a)) signify the underneath crystal lattice structure and breakdown of membrane theory.

For $q \rightarrow 0$, $\omega_{mean} \rightarrow 0$ and $\omega_{fluc} \rightarrow \sqrt{\frac{2\sigma}{\rho}}$; We identify ω_{fluc} as the LBM frequency (ZO') of a BL system. This *dispersion-less* feature of ω_{fluc} help us in two significant ways : (i) We can estimate σ directly from the flat region of $\delta H^{BL}(q)$, without depending on any other mechanical parameters. (ii) The mapping of the BL system to linear chain model (Fig.1(b)) becomes transparent. In such a model, the force constants are determined solely from the interlayer coupling. The schematics of the modes of the constituent layers at the Γ point are shown in the inset of Fig.1(a). The interlayer interaction lifts the degeneracy of the flexural modes of each layer into ω_{mean} and ω_{fluc} for $q \rightarrow 0$. This can be confirmed from the differences of $\delta H^{BL}(q)/N$ and $H^{BL}(q)/N$. In table I, we show the force constants for BL graphene and MoS₂ and compare those with the values obtained from first principles calculations. As can be easily examined from the table, our results are in excellent agreement with earlier reports.

TABLE I. Comparison of force constants calculated from MD simulation and first principles approach.

BL system	Temperature	σ ($\times 10^{19}$ N m ⁻³)	Method
Graphene	300 K	8.1	REBO + LJ
		7.3	LCBOP
Graphene	0 K	7.9	DFPT [22]
MoS ₂	300 K	8.3	SW + LJ
MoS ₂	0 K	9.26	DFPT [10]

The generalization of LBMs from BL to few layer (FL) system, can be done in similar fashion as in Eqn.(1). Keeping only the nearest neighbor layer coupling terms in FL system, we find the normalized eigenvectors and use them to compute all the height correlation

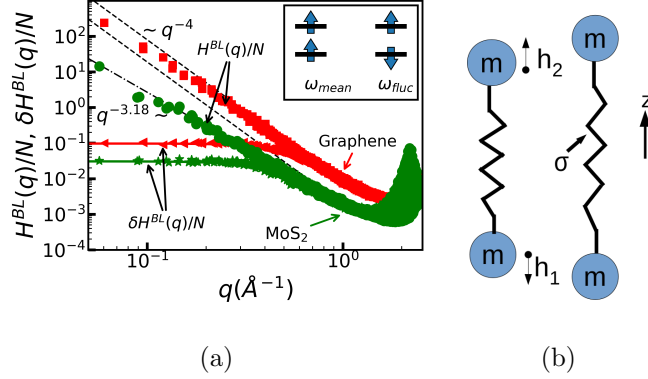


FIG. 1. (a) Height correlation functions for the *mean* mode, $H^{BL}(q)/N$ (graphene : red square, MoS₂ : green circle) and *fluctuation* mode, $\delta H^{BL}(q)/N$ (graphene : red triangle, MoS₂ : green star) for BL graphene and BL MoS₂. Black dashed and dash-dotted line show scaling q^{-4} , $q^{-3.18}$ respectively. The solid lines denote fit to the *fluctuation* mode. The inset shows schematic of normal modes at the Γ point. (b) The linear chain model : two masses (m) connected by a spring with spring constant σ .

functions *explicitly* [See SI, section C, D]. We find, the *mean* mode of FL system behaves like a single layer, for the studied sample sizes. Similar to the case of BL system, the *fluctuation* modes are identified with LBMs. In Fig.2 we show the layer dependence of LBM frequencies for graphene, MoS₂ and hBN. For a n layer system, there are $(n-1)$ distinct LBM frequencies. As can be seen from the figures, our results for graphene (Fig.2(a)) and MoS₂ (Fig.2(b)) capture the layer dependence accurately. The figures also show LBM frequencies using DFPT [10, 22]. Experimental data for graphene are shown only for the lowest LBM frequency as they dominate the Raman response [6]. The LBM with lowest frequency display an extraordinarily simple structure, where constituent layers expand and compress with respect to the mid-layer (odd n) or mid-point (even n). Qualitatively, this mode results to least restoring force, hence, lowest frequency (For schematics see SI, section D.1). With Dreiding, the frequencies are overestimated by $\sim 28\%$ (Fig.2(c)) for FL graphene. Although overestimated, the general trend for the thickness dependence of LBM frequencies is similar for hBN and graphene, consistent with another prediction [36]. We can't compare the LBM frequencies for hBN with the experimental data, as LBMs have not been characterized for hBN yet.

Two simple traits of the evolution of frequencies with thickness of 2D samples must be

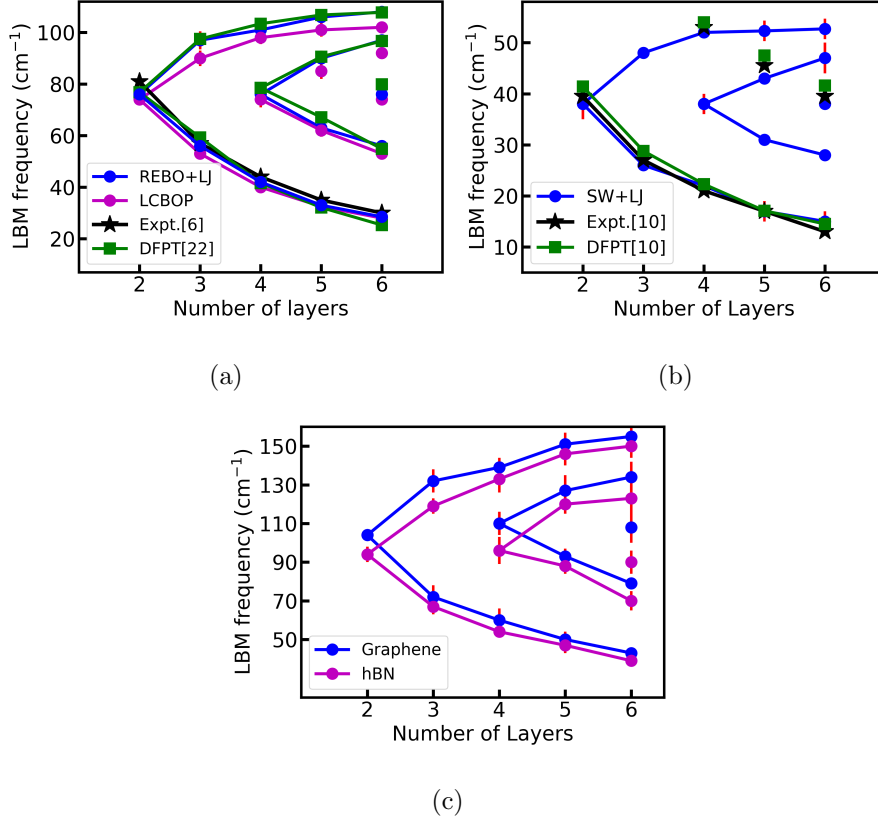


FIG. 2. Thickness dependence of LBM frequencies. (a) FL graphene (b) FL MoS₂ (c) Comparison of FL graphene and FL hBN calculated using Dreiding [27] forcefield. Solid lines are used as a guide to the eye. Vertical lines (red) denote error bars.

pointed out : (i) Upon increasing the number of layers, interlayer coupling between nearest neighbor layers remain almost constant (within the error bar), consistent with earlier report [22]. Thus, by computing σ from BL system and using a simple linear chain model the dramatic redshifts of lowest frequency of LBMs with thickness can be captured, *without calculating explicitly* the height fluctuation modes for FL sample. (ii) The effect of next-nearest neighbor interaction, is found to be negligible, for all the simulated samples (see SI, section C.1). If the coupling is significant enough, this method can be easily applied by adding more terms to the bending energy and reevaluating the height fluctuation correlations with normalized eigenvectors.

So far, in the bending energy cost (Eqn.1) for a BL system, both the interlayer and intralayer interaction terms are assumed to be harmonic. As is well known, at constant P , upon heating the material, the volume changes. This change in volume can be explained via

inclusion of anharmonic terms in the Hamiltonian. Also the change of phonon frequency (ω) with T can only be obtained from the anharmonicities of the potential energy. We calculate the change of LBM frequency with T , $\chi = \frac{d\omega}{dT}$, the first order temperature coefficient, to discern the anharmonic effects in the interlayer interaction. In this regard, we also compute the change of interlayer separation with T , $\alpha_{\perp} = \frac{1}{c} \frac{dc}{dT}$. All the reported values are estimated for BL system, with T well below the melting point.

Fig.3 shows the temperature dependence of interlayer separation and LBM frequency for BL graphene with REBO+LJ and Dreiding FF. Our results show that the equilibrium spacing between layers, c increases with T ($\alpha_{\perp} > 0$). Moreover, increasing T leads to the softening of the *effective spring constant*, σ of the harmonic oscillator. This results a redshift ($\chi < 0$) of the LBM frequency, which can also be substantiated from table II. All the anharmonic effects are automatically included in our calculation of σ . In principle, χ can be grouped into two parts : “self energy” shift due to direct anharmonic coupling of the phonon modes, χ_V and shift because of the volume change of the material, χ_T [13, 37]. As all our simulations are carried out at constant P , both contributions are included in the estimated χ . The second order temperature coefficient is found to be irrelevant in the studied temperature range. In table II, we have shown α_{\perp} , for BL systems and compared it to the bulk values [38]. With standard Dreiding parameters α_{\perp} is always underestimated compared to more accurate FFs. We find that α_{\perp} for BL (with accurate FFs) is larger than that of the bulk (experiments). It is interesting to note that there is a difference in order of magnitude for α_{\perp} ($\sim 10^{-5} \text{ K}^{-1}$) and the in-plane expansion coefficient, α_{\parallel} ($\sim 10^{-6} \text{ K}^{-1}$). This is consistent with earlier observations [39, 40]. However, the fact that α_{\perp} is greater than α_{\parallel} is not very surprising. This is due to the difference in strengths of interlayer and intralayer interactions of 2D materials.

In summary, we have analyzed out of plane vibrations of 2D materials using a combination of classical molecular dynamics simulations and membrane theory. We report our results for three different classes of 2D materials, namely, graphene, MoS₂, hBN. We provide, a consistent way to map LBMs of few layers of stacked 2D materials to a simple linear chain model in the long-wavelength limit. The thickness sensitivity of LBM frequencies at the Γ point, are well captured and in agreement with earlier reports. We also find, a redshift of LBM frequency upon increasing T . We compute the interlayer separation thermal expansion coefficient along with the shift in LBM frequency for BL systems. We show that with

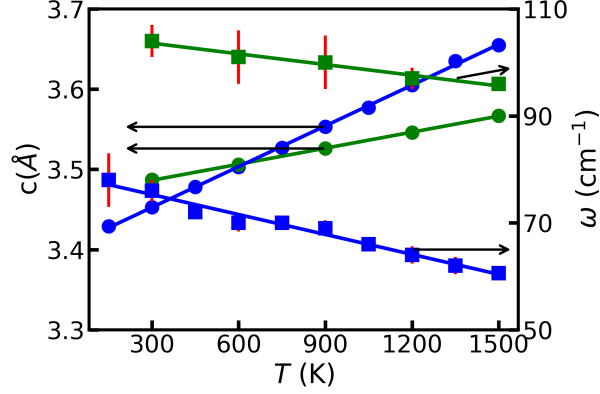


FIG. 3. Change of interlayer spacing, c (left scale) and LBM frequency, ω (right scale) with T . Blue (green) circles present variation of c using REBO+LJ (Dreiding) and blue squares (green squares) show evolution of ω using REBO+LJ (Dreiding). The solid lines represent linear fit to the data.

TABLE II. Effect of anharmonicity is to increase the interlayer spacing and redshift of LBM frequency. The thermal expansion coefficients are shown at $T = 300\text{K}$.

Material	Method	α_{\perp} ($\times 10^{-5} \text{ K}^{-1}$)	χ ($\times 10^{-3} \text{ cm}^{-1} \text{ K}^{-1}$)
BL Graphene	REBO+LJ	4.9 ± 0.2	-12.4 ± 0.8
	Dreiding	1.9 ± 0.1	-6 ± 1
	LCBOP	6.2 ± 0.3	-22.6 ± 0.9
Graphite	Expt. [41]	2.7	-
BL MoS ₂	SW+LJ	2.4 ± 0.3	-9.4 ± 1.4
Bulk MoS ₂	DFPT [42]	1.1	-
BL hBN	Dreiding	2.3 ± 0.1	-6.7 ± 0.8
Bulk hBN	Expt. [40]	3.77	-

accurate FFs LBM frequencies can be reliably estimated within this simple picture. Our method also provides a framework to capture pressure or any other external environmental effects on LBM frequencies. This study opens up the possibility of efficiently computing LBM frequencies (including anharmonic effects) to characterize and understand properties of 2D materials and their heterostructures.

The authors thank the Supercomputer Education and Research Center (SERC) at IISc for providing computational resources. The authors also thank Gaurav Kumar Gupta for

comments on the manuscript.

* mjain@iisc.ac.in

- [1] K. S. Novoselov, V. Fal, L. Colombo, P. Gellert, M. Schwab, K. Kim, *et al.*, Nature **490**, 192 (2012).
- [2] S. Z. Butler, S. M. Hollen, L. Cao, Y. Cui, J. A. Gupta, H. R. Gutiérrez, T. F. Heinz, S. S. Hong, J. Huang, A. F. Ismach, *et al.*, ACS Nano **7**, 2898 (2013).
- [3] A. K. Geim and I. V. Grigorieva, Nature **499**, 419 (2013).
- [4] P. Tan, W. Han, W. Zhao, Z. Wu, K. Chang, H. Wang, Y. Wang, N. Bonini, N. Marzari, N. Pugno, *et al.*, Nature materials **11**, 294 (2012).
- [5] L. Liang, J. Zhang, B. G. Sumpter, Q.-H. Tan, P.-H. Tan, and V. Meunier, ACS Nano **11**, 11777 (2017).
- [6] C. H. Lui, Z. Ye, C. Keiser, X. Xiao, and R. He, Nano Letters **14**, 4615 (2014).
- [7] C. H. Lui and T. F. Heinz, Physical Review B **87**, 121404 (2013).
- [8] R. He, T.-F. Chung, C. Delaney, C. Keiser, L. A. Jauregui, P. M. Shand, C. Chancey, Y. Wang, J. Bao, and Y. P. Chen, Nano Letters **13**, 3594 (2013).
- [9] X. Zhang, W. Han, J. Wu, S. Milana, Y. Lu, Q. Li, A. Ferrari, and P. Tan, Physical Review B **87**, 115413 (2013).
- [10] Y. Zhao, X. Luo, H. Li, J. Zhang, P. T. Araujo, C. K. Gan, J. Wu, H. Zhang, S. Y. Quek, M. S. Dresselhaus, *et al.*, Nano Letters **13**, 1007 (2013).
- [11] M. Boukhicha, M. Calandra, M.-A. Measson, O. Lancry, and A. Shukla, Physical Review B **87**, 195316 (2013).
- [12] J. Yan, J. Xia, X. Wang, L. Liu, J.-L. Kuo, B. K. Tay, S. Chen, W. Zhou, Z. Liu, and Z. X. Shen, Nano Letters **15**, 8155 (2015).
- [13] X. Ling, L. Liang, S. Huang, A. A. Puretzky, D. B. Geohegan, B. G. Sumpter, J. Kong, V. Meunier, and M. S. Dresselhaus, Nano Letters **15**, 4080 (2015).
- [14] Y. Zhao, X. Luo, J. Zhang, J. Wu, X. Bai, M. Wang, J. Jia, H. Peng, Z. Liu, S. Y. Quek, *et al.*, Physical Review B **90**, 245428 (2014).
- [15] H. Li, J.-B. Wu, F. Ran, M.-L. Lin, X.-L. Liu, Y. Zhao, X. Lu, Q. Xiong, J. Zhang, W. Huang, H. Zhang, and P.-H. Tan, ACS Nano **11**, 11714 (2017).

- [16] R. He, J. van Baren, J.-A. Yan, X. Xi, Z. Ye, G. Ye, I.-H. Lu, S. Leong, and C. Lui, *2D Materials* **3**, 031008 (2016).
- [17] R. He, J.-A. Yan, Z. Yin, Z. Ye, G. Ye, J. Cheng, J. Li, and C. Lui, *Nano Letters* **16**, 1404 (2016).
- [18] C. H. Lui, Z. Ye, C. Ji, K.-C. Chiu, C.-T. Chou, T. I. Andersen, C. Means-Shively, H. Anderson, J.-M. Wu, T. Kidd, *et al.*, *Physical Review B* **91**, 165403 (2015).
- [19] V. Perebeinos, J. Tersoff, and P. Avouris, *Physical Review Letters* **109**, 236604 (2012).
- [20] P. S. Mahapatra, K. Sarkar, H. R. Krishnamurthy, S. Mukerjee, and A. Ghosh, *Nano Letters* **17**, 6822 (2017).
- [21] There is no periodicity in the out of plane (z) direction of FL system. $\Gamma - A$ branch of the bulk counterpart is non existent in the Brillouin zone (BZ). One can show, the frequencies of LBMs at Γ point for FL system, are associated with vibrations of their bulk correspondent along $\Gamma - A$ direction.
- [22] S. K. Saha, U. Waghmare, H. Krishnamurthy, and A. Sood, *Physical Review B* **78**, 165421 (2008).
- [23] S. Plimpton, *Journal of Computational Physics* **117**, 1 (1995).
- [24] J. Los and A. Fasolino, *Physical Review B* **68**, 024107 (2003).
- [25] D. W. Brenner, O. A. Shenderova, J. A. Harrison, S. J. Stuart, B. Ni, and S. B. Sinnott, *Journal of Physics: Condensed Matter* **14**, 783 (2002).
- [26] L. Girifalco, M. Hodak, and R. S. Lee, *Physical Review B* **62**, 13104 (2000).
- [27] S. L. Mayo, B. D. Olafson, and W. A. Goddard, *Journal of Physical Chemistry* **94**, 8897 (1990).
- [28] J.-W. Jiang, H. S. Park, and T. Rabczuk, *Journal of Applied Physics* **114**, 064307 (2013).
- [29] T. Liang, S. R. Phillpot, and S. B. Sinnott, *Physical Review B* **79**, 245110 (2009).
- [30] T. Liang, S. R. Phillpot, and S. B. Sinnott, *Physical Review B* **85**, 199903 (2012).
- [31] D. Nelson, T. Piran, and S. Weinberg, *Statistical mechanics of membranes and surfaces* (World Scientific, 2004).
- [32] A. Fasolino, J. Los, and M. I. Katsnelson, *Nature Materials* **6**, 858 (2007).
- [33] B. Amorim, R. Roldán, E. Cappelluti, A. Fasolino, F. Guinea, and M. Katsnelson, *Physical Review B* **89**, 224307 (2014).
- [34] This is the height-height correlation in momentum space. For convenience, we write it as

height correlation function.

- [35] P. Le Doussal and L. Radzihovsky, Physical Review Letters **69**, 1209 (1992).
- [36] K. Michel and B. Verberck, Physical Review B **85**, 094303 (2012).
- [37] C. Postmus, J. R. Ferraro, and S. S. Mitra, Phys. Rev. **174**, 983 (1968).
- [38] The value of α_{\perp} and χ for MoS₂ is calculated by changing T from 150 K to 450 K only.
- [39] N. Mounet and N. Marzari, Physical Review B **71**, 205214 (2005).
- [40] W. Paszkowicz, J. Pelka, M. Knapp, T. Szyszko, and S. Podsiadlo, Applied Physics A **75**, 431 (2002).
- [41] A. Bailey and B. Yates, Journal of Applied Physics **41**, 5088 (1970).
- [42] C. K. Gan and Y. Y. F. Liu, Physical Review B **94**, 134303 (2016).